Optimization of Line Cut Strategy for Bone Tissue Ablation Using Short-Pulsed CO_2 Laser Based on Thermal Relaxation

Y. Zhang, J. Burgner, J. Raczkowsky, H. Wörn

Karlsruhe Institute of Technology (KIT), Institute for Process Control and Robotics (IPR), Karlsruhe, Germany

Contact: yaokun.zhang@kit.edu

Abstract:

In order to keep a low degree of thermal injury to the target tissue, the traditional line cut strategy of laser osteotomy has limited the applied pulse repetition rate to be under certain threshold, which results in a very long temporal duration of the cutting procedure. Based on the analysis of the post-pulse thermal relaxation behavior inside the tissue surrounding the ablation crater, a "jumping cut strategy" is developed in this paper. Experimental evaluation has shown that this new strategy is able to accelerate the cutting procedure as well as reduce the thermal injury to the tissue at the same time.

Key Words: laser ablation, thermal relaxation, hard tissue processing

1 Motivation

In the last decade, the feasibility of the processing hard tissue (mainly bone tissue) using laser, known as laser ablation, has been studied by different authors. Short-pulsed CO_2 laser has been considered as an excellent tool for laser osteotomy [1-3]. Due to the strong absorption of the incident energy through the mineral component (hydroxyapatite) of bone tissue, the heat deposition in the irradiated tissue can be confined in a very small volume. This leads to a rapid increase of the local temperature and results in a micro-explosion, which ablates a tiny piece of tissue and forms a crater on the tissue surface. Meanwhile, most of the incident energy is again brought away by the ablated particles, so that the thermal injury in the adjacent tissue is minimized [4,5]. To prevent dehydration of the tissue and further reduce the thermal damage, [5,6] have suggested to apply an extra water spray to the irradiated region.

With the help of a laser scanner, the laser spot with the radius w can be moved over the target tissue surface fast and with high repeatability. Suppose the velocity of the laser spot is v and the repetition rate of the laser pulse is f, then the distance between two pulses is Δx, so that the single pulses are overlapped with the neighbors and a line as well as a trajectory of arbitrary geometry can be induced, as illustrated in figure 1.

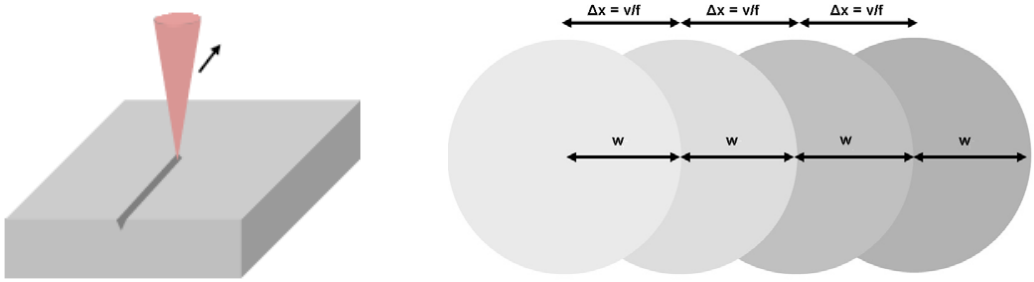

Figure 1: Illustration of (left) line cutting strategy by moving laser spot over the tissue sur 三 face [7], (right) overlap of the neighbor pulses [3].

However, despite the micro-explosion and water spray, experiments have shown that appreciable carbonization of the adjacent tissue surrounding the incision can still occur if the pulse repetition rate is too high. In such a case, the tissue surrounding the crater ablated by the first pulse will not have enough time to b cool down before the second neighbor pulse is applied, so that the residual heat after the ablation will be accumulated in the adjacent tissue and results in a severe thermal damage. Therefore, [3,7] have limited the repetition rate to 200Hz and [5] has conducted the experiments with 50-400Hz. For animal experimentation, even lower repetition rates (<10Hz) are chosen by the authors [8-10].

However, limiting the repetition rate also increases the temporal duration of the cutting procedure. For example, cutting of a 1cm x 1cm square block on a 5mm thick bone specimen costs about 1 hour with 200Hz repetition rate, which increases the risk of the surgical operation and is unacceptable for the clinical application. Nevertheless, laser ablation promises high cutting accuracies and cutting width unachievable with conventional technologies [11]. Hence, optimization is required.

2 Methods

To avoid the heat accumulation inside the tissue, a new cutting strategy has been developed. The basic idea is very simple: instead of sequential order, the pulses composing the trajectory are divided into several rounds and any two pulses of the same round have to hold a minimal distance to each other, so that the heat diffusion surrounding them will not affect each other. Such a distance is called as *safety-distance*, noted as d_s. Obviously, d_s is not necessarily an integral multiple of the spot radius w. Therefore, another parameter *jumping-distance* n_j is defined as the following equation, which gives explicit the number of craters to be skipped between two neighbor craters of the same round:

$$n_j = \left\lceil \frac{d_s}{w} \right\rceil \tag{1}$$

where the ceil function $\lceil \cdot \rceil$ denotes the smallest integer that is larger than or equals the operand.

Knowing the jumping-distance, the craters will be equally divided into exactly n_j rounds. Figure 2 illustrates an example with $n_j = 5$, so that the craters composing the line in the top are divided into rounds A to E. The sequence of the ablation is then $A_1, A_2, \cdots, B_1, B_2, \cdots, E_1, E_2 \cdots$. Actually, the conventional sequential line cut strategy can be regarded as a special case of jumping cut strategy with $n_j = 1$.

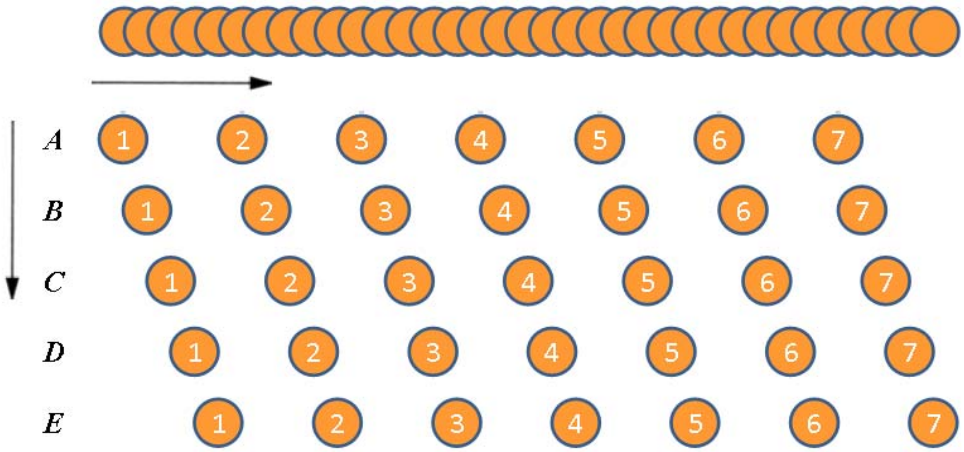

Figure 2: Illustration of jumping cut strategy.

If the pulse repetition rate f is chosen properly, by the time the round A is finished, the adjacent tissue surrounding the crater A_1 has already been cooled to a safe temperature, so that the pulse B_1 can be applied without bringing extra thermal injury due to heat accumulation.

Suppose each round contains m craters. Obviously, each single pulse consumes a time period of f^{-1} and each round costs hence mf^{-1}. The time it needs for the adjacent tissue to be cooled is called as *thermal decay time*, noted as t_d. Then, the following relation must be satisfied in order to prevent heat accumulation:

$$f \le \frac{m}{t_d} = \frac{n}{n_j \cdot t_d} = \frac{n}{t_d} \cdot \left\lceil \frac{d_s}{w} \right\rceil^{-1} \tag{2}$$

where $n = m \cdot n_j$ is the total number of the craters in the line. Consequently, the only question is to determine the safety-distance d_s and thermal decay time t_d, which can be obtained by simulating the post-pulse thermal relaxation inside the tissue surrounding each crater.

After each pulse, no more energy will be deposited in the irradiated tissue, i.e. there exists no more heat source in the tissue. Hence, the change of temperature can be described by homogeneous heat conduction equation

$$\dot{T} = \frac{k}{\rho c} \nabla^2 T$$

where k is the thermal conductivity, ρ the mass density and c the specific heat capacity of the bone tissue, T the tem-

perature and ∇^2 the Laplace operator . Consider the irradiated volume as a cylinder, then this heat conduction equation can be written as

$$\frac{\partial T}{\partial t} = \frac{k}{\rho c}\left(\frac{\partial^2}{\partial r^2} + \frac{1}{r}\frac{\partial}{\partial r} + \frac{\partial^2}{\partial z^2}\right)T \qquad (3)$$

where t denotes the time, (r, z) is the cylindrical coordinate of any point in the irradiated volume. With the help of the discrete form of equation (3), the temperature of any point (r, z) at any time point t can be numerical simulated. Figure 3 shows the result of simulation at different time points as example, where the incident laser is Gaussian beam, pulsed energy is 22.4mJ, pulse duration 80 µs, beam waist spot radius 99 µm and k=0.4W/(m·K), ρ=2g/cm^3, c=1.3J/(g·K).

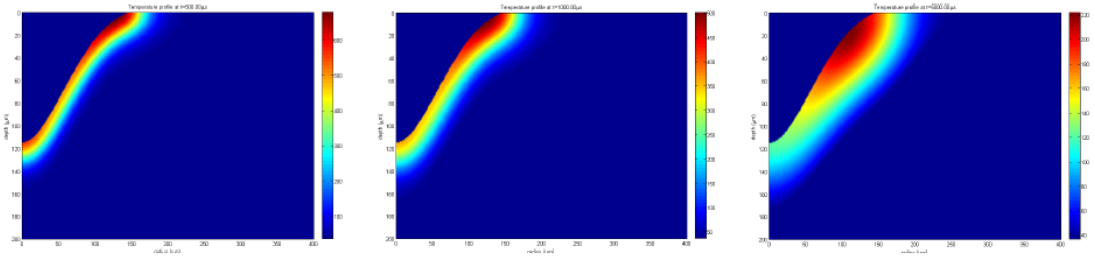

Figure 3: Simulated post-pulse heat diffusion in the tissue surrounding the ablation crater at t=500, 1000, 5000 µs.

For biological tissues, 60 °C and 42 °C are two critical temperatures: above 60 °C, denaturation of proteins and coagulation may occur after an exposure of several seconds; under 42 °C, no injury can be observed, no matter how long the temporal duration is [12]. Considering the body temperature and the overlap of neighbor pulses, 48.5 °C, 39.5 °C and 37.5 °C are chosen as threshold temperatures. Hereby 37.5 °C is chosen instead of 37 °C in order to shorten the duration of the simulation. Analyze the result of the simulation, the thermal decay time t_d and safety-distance d_s corresponding the different thresholds can be determined and are listed in table 1.

focus distance	spot radius [µm]	thermal decay time [ms]			safety-distance [µm]		
		48.5 °C	39.5 °C	37.5 °C	48.5 °C	39.5 °C	37.5 °C
0	99	28.05	41.92	57.56	340	377	456
$0.25z_R$	102	28.74	42.93	58.95	349	386	467
$0.50z_R$	111	30.69	45.76	62.79	373	413	498
$0.75z_R$	124	33.34	49.62	68.02	407	452	541
z_R	140	36.08	53.59	73.40	446	496	592

Table 1: Thermal decay time and safety-distance. Focus distance denotes the distance from the tissue surface to the beam waist, where z_R is the Rayleigh range.

3 Results

Substitute the simulated thermal decay time t_d and safety-distance d_s into equations (1) and (2), the jumping-distance n_j and the maximal allowed pulse repetition rate f can be obtained. The results show that at any focus distances, the safety-distances determined with 48.5 °C, 39.5 °C are corresponded to the jumping-distance 4 and the other one yields n_j=5. Consequently, at each focus distance, there exist six combinations of f and n_j.

The new strategy is then evaluated by etching straight lines on fresh bovine compact bone. The three different thermal decay times are corresponded to the pulse repetition rate of 1737, 2385 and 3565Hz respectively. Considering the different thermal decay times at different focus distances, the repetition rate 1000Hz, which satisfies the relation (2) for any focus distances within the Rayleigh range, is also tested. The resulted incisions are observed under microscope, as shown in figure 4.

For comparison, the conventional sequential cutting strategy with repetition rate 1Hz and 200Hz are applied on the same specimen. It can be concluded that the degree of carbonization in the incisions etched with the new strategy is obviously lighter than that of the sequential one.

Notice that the new strategy only changes the sequence of the pulse distribution. Therefore, the cutting efficiency is proportional to the pulse repetition rate. Consequently, the jumping cut strategy has achieved to accelerate the cutting procedure up to ca. 17 times as well as reduce the degree of thermal injury to the tissue at the same time.

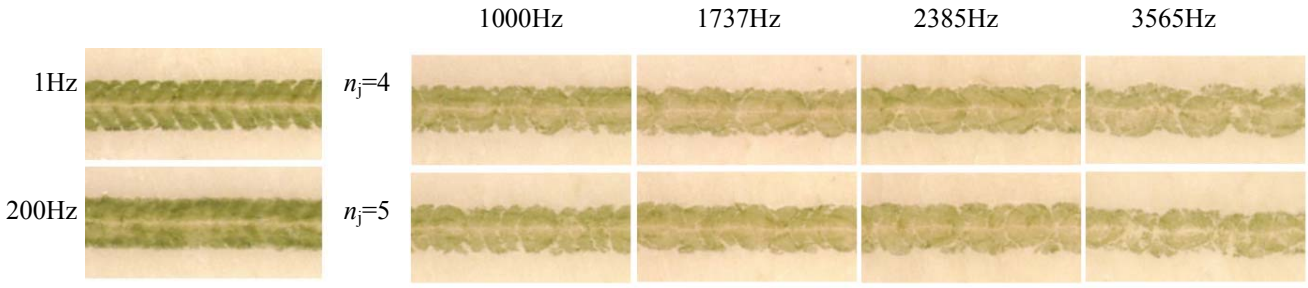

Figure 4: Evaluation of jumping cut strategy. (left) reference incision etched with sequential cutting strategy, (right) incision etched with jumping cut strategy with different jumping-distance and pulse repetition rate.

4 Disscussion

The two key parameters of the jumping cut strategy, namely thermal decay time and safety-distance, are dependent on the chosen threshold temperature. For the first two thresholds 48.5°C and 39.5°C, the tissue is actually not totally cooled before the second pulse is applied, so that it can still occur, that the residual heat accumulates after several pulses. Therefore, the priority of the three thresholds should be 48.5°C< 39.5°C< 37.5°C.

According to the relation (2), the more craters a trajectory contains, the higher repetition rate is allowed. In other words, for a trajectory with very little craters, for example less than 50 craters, the cutting efficiency will be reduced. Because by the time the round *A* is finished, the tissue surrounding crater A_1 is still not cooled, so that the round *B* has to be delayed. In such a case, a trade-off between pulse frequency and threshold temperature should be made and a higher threshold temperature could be chosen in order to accelerate the cutting procedure.

From figure 4, it can also be seen that the degree of carbonization even decreases with the repetition rate. One possible reason for such a result might be so explained that at higher repetition rate, the power out put of the laser source becomes unstable and the energy of each single pulse is reduced. However, for the repetition rate 1737Hz, the power output is only about 40W, while the available power is 100W, but this phenomenon can be still observed. A further systematic study on this phenomenon is needed for a more reasonable explanation.

It should also be noticed that the evaluation of the new strategy is currently limited to comparing the degree of carbonization inside the resulted incision. A further histological study on other thermal injuries such as coagulation will make the conclusion more convincing. The experimental setup introduced in [3], which uses an infrared camera to monitor the specimen temperature, also provides another way for the evaluation.

For the future work, the jumping cut strategy can be further enhanced with an “interlaced jumping cut strategy”. For example, the rounds *A*· · ·*E* given in figure 2 can be ablated in the sequence *A,C,E,B,D* instead of *A,B,C,D,E*. Because the distance between the crater A_1 and C_1 is larger than that between A_1 and B_1, the round *C* can be applied earlier than round *B*, which can therefore further increase the repetition rate. With proper adaption, the jumping cut strategy can also be available for processing of a large surface instead of only cut a trajectory.

5 Bibliography

[1] Thomas Mitra. *Ablation biologischen Hartgewebes mit gepulsten IR-Lasern*. Doctoral thesis, Universität Düsseldorf, 2002.

[2] Said Afilal. *Ablationsmechanismen von biologischem Hartgewebe bei Bestrahlung mit kurzgepulsten CO_2-Lasern*. Doctoral thesis, Heinrich-Heine-Universität Düsseldorf, 2004.

[3] Martin Werner. *Ablation of hard biological tissue and osteotomy with pulsed CO_2 lasers*. Doctoral thesis, University Düsseldorf, 2006.

[4] Alfred Vogel and Vasan Venugopalan. Mechanisms of Pulsed Laser Ablation of Biological Tissues. *Chemical Review*, 2003.

[5] Martin Werner, Mikhail Ivanenko, Daniela Harbecke, Manfred Klasing, Hendrik Steigerwald and Peter Hering. CO_2 laser “milling” of hard tissue. *Proc. of SPIE Vol. 6435, 64350E*, 2007.

[6] M.M. Ivanenko, P. Hering. Wet bone ablation with mechanically Q-switched high-repetition-rate CO_2 laser. *Applied Physics B: Lasers and Optics*, Bd. 67(3):395–397, 1998.
[7] Jessica Burgner. *Robot Assisted Laser Osteotomy*. Doctoral thesis, Karlsruhe Institute of Technology, 2010.
[8] J. S. Nelson, A. Orenstein, L.-H. L. Liaw, and M.W. Berns. Mid-infrared erbium:YAG laser ablation of bone: The effect of laser osteotomy on bone healing. *Lasers in Surgery and Medicine*, vol. 9, pp. 362–374, 1989.
[9] Buchelt, H. Kutschera, T. Katterschafka, H. KIss, S. Lang, R. Beer, and U. Losert. Erb:YAG and Hol:YAG Laser Osteotomy: The Effect of Laser Ablation on Bone Healing. *Lasers in Surgery and Medicine,* vol. 15, pp. 373–381, 1994.
[10] J. Payne, G. Peavy, L. Reinisch, and D. Van Sickle. Cortical Bone Healing Following Laser Osteotomy Using 6.1 μm Wavelength. *Lasers in Surgery and Medicine*, vol. 29, pp. 38–43, 2001.
[11] J. Burgner, M. Müller, J. Raczkowsky, H. Wörn. Robot assisted laser bone processing: Marking and cutting experiments. *14th International Conference on Advanced Robotics (ICAR),* 2009
[12] Markolf H. Niemz. *Laser-Tissue Interactions: Fundamentals and Applications*. Springer, third, enlarged edition , 2007.